Journal of Visualized Experiments

Quantifying Spatiotemporal Parameters of Cellular Exocytosis in Micropatterned Cells

--Manuscript Draft--

Article Type:	Invited Methods Article - JoVE Produced Video
Manuscript Number:	JoVE60801R2
Full Title:	Quantifying Spatiotemporal Parameters of Cellular Exocytosis in Micropatterned Cells
Section/Category:	JoVE Biology
Keywords:	Lysosomes, Organelles, secretion, micropatterning, statistical analysis, TIRF microscopy
Corresponding Author:	Kristine Schauer Centre National de la Recherche Scientifique Paris, Paris FRANCE
Corresponding Author's Institution:	Centre National de la Recherche Scientifique
Corresponding Author E-Mail:	kristine.schauer@curie.fr
Order of Authors:	Kristine Schauer
	Hugo Lachuer
	Pallavi Mathur
	Kevin Bleakley
Additional Information:	
Question	**Response**
Please indicate whether this article will be Standard Access or Open Access.	Standard Access (US$2,400)
Please indicate the **city, state/province, and country** where this article will be **filmed**. Please do not use abbreviations.	Paris, France

Powered by Editorial Manager® and ProduXion Manager® from Aries Systems Corporation

Manuscript Click here to access/download;Manuscript;60801_R2.docx

TITLE:

Quantifying Spatiotemporal Parameters of Cellular Exocytosis in Micropatterned Cells

AUTHORS AND AFFILIATIONS:

Hugo Lachuer[1,2], Pallavi Mathur[1,2], Kevin Bleakley[3], Kristine Schauer[1,2]

[1]Institut Curie, Unité Mixte de Recherche 144, Molecular Mechanisms of Intracellular Transport group, 75005 Paris, France

[2]Sorbonne Université, Collège Doctoral, F-75005 Paris, France

[3]INRIA, Université Paris-Sud, 91405 Orsay Cedex, France

Corresponding Author:

Kristine Schauer (kristine.schauer@curie.fr)

Email Addresses of Co-authors:

Hugo Lachuer (hugo.lachuer@curie.fr)

Pallavi Mathur (pallavi.mathur@curie.fr)

Kevin Bleakley (kevbleakley@gmail.com)

KEYWORDS:

micropattern, lysosome, exocytosis, TIRFM, CSR, VAMP7

SUMMARY:

Live imaging of lysosomal exocytosis on micropatterned cells allows a spatial quantification of this process. Morphology normalization using micropatterns is an outstanding tool to uncover general rules about the spatial distribution of cellular processes.

ABSTRACT:

Live imaging of the pHluorin tagged Soluble N-ethylmaleimide-sensitive-factor Attachment protein REceptor (v-SNARE) Vesicle-associated membrane protein 7 (VAMP7) by total internal reflection fluorescence microscopy (TIRFM) is a straightforward way to explore secretion from the lysosomal compartment. Taking advantage of cell culture on micropatterned surfaces to normalize cell shape, a variety of statistical tools were employed to perform a spatial analysis of secretory patterns. Using Ripley's K function and a statistical test based on the nearest neighbor distance (NND), we confirmed that secretion from lysosomes is not a random process but shows significant clustering. Of note, our analysis revealed that exocytosis events are also clustered in nonadhesion areas, indicating that adhesion molecules are not the only structures that can induce secretory hot spots at the plasma membrane. Still, we found that cell adhesion enhances clustering. In addition to precisely defined adhesive and nonadhesive areas, the circular geometry of these micropatterns allows the use of polar coordinates, simplifying analyses. We used Kernel Density Estimation (KDE) and the cumulative distribution function on polar coordinates of exocytosis events to identify enriched areas of exocytosis. In ring-shaped micropattern cells, clustering occurred at the border between the adhesive and nonadhesive

areas. Our analysis illustrates how statistical tools can be employed to investigate spatial distributions of diverse biological processes.

INTRODUCTION:

Exocytosis is a universal cellular process in which a vesicle fuses with the plasma membrane and releases its content. The vesicle can either fuse totally with the plasma membrane (full fusion) or create a fusion pore that stays open during a limited time (kiss-and-run)[1]. For instance, newly synthesized proteins are released into the extracellular medium from vesicles that come from the Golgi complex. This biosynthetic, anterograde pathway is primordial, especially in multicellular organisms, to secrete signaling peptides (e.g., hormones, neurotransmitters) and extracellular matrix components (e.g., collagen), as well as to traffic transmembrane proteins to the plasma membrane. Additionally, secretions can occur from different endosomes: 1) recycling endosomes in order to reuse transmembrane proteins; 2) multivesicular bodies (MVBs) to release exosomes; and 3) lysosomes for the release of proteolytic enzymes. Endosomal secretion has been shown to be important for neurite outgrowth, pseudopodia formation, plasma membrane repair, and ATP-dependent signaling[2].

To study exocytosis at the single cell level, several techniques have been employed. Patch-clamp allows for the detection of single exocytosis events with a high temporal resolution in a wide variety of living cells[3]. However, this method does not provide information on the localization of exocytosis events, nor from which compartment it occurs. Electron microscopy allows direct visualization of exocytic events with high spatial resolution, and in combination with immunolabeling provides information about the specificity of the compartments and molecules involved. A disadvantage of this approach is the lack of information on the dynamics of the process, as well as its inability to perform high-throughput studies. Light microscopy approaches such as total internal reflection fluorescence microscopy (TIRFM), which exploits the evanescent field to illuminate fluorophores at the vicinity of the coverslip (100 nm), provides good temporal and spatial resolution to study exocytosis events. However, this method is only compatible with adherent cells and can only be applied to the ventral/inferior part of cells.

Of note, the plasma membrane reveals significant heterogeneity based on adhesive complexes that are present only in restricted areas. This heterogeneity restricts, for instance, the uptake of different ligands[4]. Similarly, it has recently been reported that secretion from the Golgi complex is concentrated at “hot spots” in the plasma membrane[5]. Moreover, it is known that certain cargos are secreted through focal-adhesion-associated exocytosis[6]. Thus, special attention should be paid to the question of whether exocytosis events are randomly distributed in space, or whether they are concentrated at specific areas of the plasma membrane. Several statistical tools based on Ripley’s K function have been proposed to explore these questions[7,8,9]. Our approach combines these tools with micropatterning to control cell shape and plasma membrane heterogeneity. In addition to providing a means to distinguish between adhesive and nonadhesive areas, this technique also allows comparison across different cells and conditions and increases the power of statistical analyses.

Here we employ a variety of statistical tools to study the spatial distribution of exocytosis events from the lysosomal compartment monitored by TIRFM live cell imaging of VAMP7-pHluorin in ring-shaped micropattern-normalized hTert-RPE1 cells. It was confirmed that secretion from lysosomes is not a random process[8,9] and that exocytosis events exhibit clustering. Of note, we found that exocytosis events are also clustered in nonadhesive areas, indicating that adhesion molecules are not the only structures that can induce secretory hot spots at the plasma membrane. Nevertheless, cell adhesion did enhance clustering. Consistently, our analysis identified enriched areas of exocytosis that were located at the border between the adhesive and nonadhesive areas.

PROTOCOL:

1. Preparation of micropatterned cells

1.1. Transfection of cells

1.1.1. One day before transfection, seed 2.5 x 10^6 hTERT-RPE1 cells into one well of a 12 well plate (2 x 2 cm) in 1 mL of medium.

1.1.2. On the day of transfection, prepare the transfection mixture with VAMP7-pHluorin plasmid (100 µL of buffer, 0.8 µg of DNA, 3 µL of transfection mixture). Incubate for 10 min.

NOTE: VAMP7 is a lysosomal v-SNARE, fused with a luminal pHluorin tag. The pHluorin probe is quenched by low pH, but during exocytosis protons are released and pHluorin starts emitting a signal[10,11].

1.1.3. Add the transfection mix to the cells in their medium.

1.1.4. Change the medium 4 h after adding the transfection mix on the cells.

1.1.5. Use the cells for experiments during the next 24–48 h.

1.2. Micropattern preparation (photolithography method)

1.2.1. Wash the coverslips (22 x 22 mm) in ethanol and let them dry for 5 min.

1.2.2. Activate coverslips by illumination under deep UV for 5 min.

1.2.3. Create a humid chamber by thoroughly humidifying a paper towel on which a paraffin film is placed. Add drops (30 µL for 22 mm coverslip) of Poly-L-Lysine-graft-Polyethylene Glycol (PLL-g-PEG) solution (0.1 mg/mL, 10 mM HEPES, pH = 7.4) and place coverslips with the activated surface on them. Close the humid chamber with a top and incubate coverslips for 1 h.

1.2.4. Wash coverslips 2x in PBS and 1x in distilled water and let them dry.

1.2.5. Wash the quartz photomask with distilled water and then with ethanol or propanol. Dry the photomask with filtered airflow.

NOTE: The quartz photomask is coated on one side with antireflective chrome that contains holes in the form of micropatterns. A photomask containing ring-shaped micropatterns of 37 µm is used in this protocol. When deep UV is shined on the photomask, the light can only pass through these holes[12].

1.2.6. Expose the photomask (chrome-coated side) to deep UV for 5 min to clean the surface.

1.2.7. Add small water drops (10 µL for a 20 mm coverslip) on the chrome-coated side of the photomask. Place the coverslip with their PLL-g-PEG-treated side on the drop and dry the extra water. Make sure that no air bubbles form between the mask and the coverslips.

NOTE: The capillary force of the water will immobilize the coverslips.

1.2.8. Expose the photomask to deep UV for 5 min with the non-chrome-coated side up (the coverslips are attached on the lower surface).

NOTE: The light can only pass through the holes and modify the PLL-g-PEG-treated surface of coverslips below the photomask.

1.2.9. Remove the coverslips from the photomask by adding excess water.

NOTE: Coverslips should quickly float off.

1.2.10. Incubate the coverslips in a solution of extracellular matrix proteins (50 µg/mL of fibronectin, 5 µg/mL of fluorescent fibrinogen diluted in water) on paraffin film in a humid chamber (as in step 1.2.3) for 1 h under a laminar flow hood to avoid contamination.

NOTE: The experiment can be paused at this point by storing the coverslips in PBS at 4 °C.

1.3. Cell seeding on micropatterned surfaces

1.3.1. Use a magnetic coverslip holder that fits the size of the micropatterned coverslips to mount the coverslips. On the day of acquisition, heat the coverslip holder to 37 °C to avoid thermal shock for the cells during subsequent steps.

1.3.2. Prepare the pattern medium by supplementing DMEM/F12 medium with 20 mM HEPES and 2% of penicillin/streptomycin.

1.3.3. Place coverslips into the holder with the micropatterned side up and add pattern medium as soon as the coverslip is on the holder base. Add the seal and immobilize with the magnetic device. Fill the coverslip holder with the pattern medium and close it with the glass lid.

NOTE: Be quick, to not allow the coverslip to dry. Do not wash the coverslip holder with ethanol between experiments, because the seal might retain some ethanol, which can react with PLL-g-PEG and result in cell stress. Wash the coverslip holder only with soapy water. Moreover, the joint can be incubated in the pattern medium at 37 °C for 1 h to dilute residual product.

1.3.4. Collect transfected hTERT-RPE1 cells by trypsinization (0.5 mL for one 12 well plate) and add 1 mL of 10% FBS DMEM/F12 medium.

1.3.5. Add 0.5 x 10^6 transfected hTERT-RPE1 cells to the coverslip holder and reclose it. Incubate for 10 min in the incubator.

1.3.6. Wash the coverslip holder 5x with pattern medium to remove nonattached cells and residual FBS by adding the pattern medium with one pipette and aspirating the medium with another pipette to create a washing flow. Always keep a small volume of pattern medium in the coverslip holder to avoid drying of the cells on the micropatterned coverslip, which will lead to cell death.

1.3.7. Incubate in the incubator for 3 h to allow full cell spreading.

2. Acquisition of exocytosis data

2.1. Imaging of exocytosis events

2.1.1. Place coverslip holder under a TIRM. The signal has to be detected by a sensitive camera set up with the best imaging format available.

NOTE: In this experiment, a 100x lens objective and an EMCCD camera with 512 x 512 pixel detection region was used giving rise to a pixel size of 160 nm.

2.1.2. Search for a cell expressing VAMP7-pHluorin that is fully spread (**Figure 1A**).

NOTE: Cells expressing VAMP7 are clearly identifiable, because they exhibit a green signal.

2.1.3. Change the angle of the laser until a TIRF angle that allows the visualization of VAMP7-pHluorin exocytosis events is reached. Perform a 5 min acquisition at a frequency compatible with the exocytosis rate and time scale (typically 3 Hz, **Figure 1D**) using the microscope software.

NOTE: hTERT-RPE1 cells have a lysosomal secretory rate of around 0.3 Hz on micropatterns. Lysosomal exocytosis has a typical duration of 1 s. It is characterized by a peak intensity followed by an exponential decay. The diffusion of the probe should be evident at this time (**Figure 1B**, **C**).

2.1.4. For each cell, also perform an acquisition of the micropattern using the microscope software (**Figure 1A**).

2.2. Acquisition of exocytosis coordinates

2.2.1. Open the acquired movie with ImageJ/FIJI. Use **File** | **Import** | **Image Sequence**. Find exocytosis events by eye. An exocytosis event is characterized by the appearance of a bright signal that spreads outwards (**Figure 1**).

2.2.2. Use the point tool to mark the center of the exocytic event. Use **Analyze** | **Measure** to measure X and Y coordinates, as well as the temporal coordinate (slice number). Perform these measurements for all exocytosis events of the movie.

2.2.3. Save the results (**Results** | **File** | **Save As**). Prepare a text file for each analyzed cell named "Results(cell_name).txt" that contains the slice, X coordinates, and Y coordinates for all exocytosis events in that order.

The text file is supposed to look like this:

ID	X	Y	Feret's diameter	Radius
RPE1_WT_Cell1	167	136	230	115
RPE1_WT_Cell2	164	160	230	115

NOTE: Be careful to replace all commas with points.

2.2.4. Measure the center and diameter of each cell using the "**Oval Tool**". Fit a perfect circle (do not use an oval) and use "**Measure**" to obtain the X and Y coordinates and Feret's diameter. Save each cell's identity (ID), X and Y coordinates, Feret's diameter, and radius (diameter/2) in a text file named "Spherical parameter.txt".

The text file is supposed to look like this:

ID	X	Y	Feret's diameter	Radius
RPE1_WT_Cell1	167	136	230	115
RPE1_WT_Cell2	164	160	230	115

NOTE: Be careful to replace all commas with points.

2.2.5. Measure the thickness of the micropattern ring (adhesion length) with the straight tool and save the cell ID, cell radius (from the file: "Spherical parameter.txt"), and adhesion length in a text file named "Pattern parameter.txt". Calculate the normalized adhesion length by dividing the adhesion length by cell radius.

NOTE: Be careful to replace all commas by points.

The file should look like this:

ID	Cell radius	adhesion length	Normalized adhesion length
RPE1_WT_Cell1	115	34	0.295652174
RPE1_WT_Cell2	115	35	0.304347826

3. Single cell spatial analysis

3.1. R package and installation

NOTE: The R package for this analysis takes advantage of the Spatstat package[13] to compute the two-dimensional (2D) density and Ripley's K function. The code is open-source and uses text files that have been previously described.

3.1.1. Download and install R from https://www.r-project.org/ (version 3.5.2 was used in this analysis).

3.1.2. Download the package (and the demo dataset) from: https://github.com/GoudTeam/JoVE-paper

3.1.3. Install the package on R Studio using "**Tools**" using "**Install Packages**". Select "**Package Archive File (.zip; .tar.gz)**" for the category "**Install from:**" and choose the package file. Press "**Install**".

3.1.4. Load the package with the function "**library("ExocytosisSpatialAnalysis")**" by writing this command in R studio and pressing "**Enter**".

3.1.5. Run the package with the function "**ESA()**" by writing this command in R studio and pressing "**Enter**".

NOTE: A user interface will open.

3.1.6. Select the directory for the dataset (.txt files) and a directory for output plots.

NOTE: Parameters of the analysis (see text below) can be changed through a user interface.

3.1.7. This script will automatically start and perform the analysis. It provides .pdf files of corresponding plots and .txt files containing numerical results.

REPRESENTATIVE RESULTS:

The spatiotemporal characteristics of exocytosis events were analyzed from lysosomes visualized by VAMP7-pHluorin[10-11] in hTert-RPE1 cells. hTert-RPE1 cells are nontransformed cells that adopt well to micropatterning and have been extensively used in previous micropattern-based studies[4,14]. VAMP7 is a lysosomal v-SNARE[15] that was tagged with the super ecliptic pHluorin at its N-terminus and is located in the lumen of the lysosome. Inside the cell, the pHluorin probe

was quenched by the low pH of the lysosome, but during exocytosis pHluorin started to emit a signal because the pH increased due to proton release. VAMP7-pHluorin was monitored by TIRFM live cell imaging on ring-shaped micropatterns (**Figure 1A–B**). The pHluorin signal exhibited a peak during exocytosis that represented the fast release of lysosomal protons followed by exponential decay, representing the 2D diffusion of the probe at the plasma membrane (**Figure 1C**). hTERT-RPE1 cells presented an important lysosomal secretion activity with an averaged exocytosis rate of 0.28 Hz (**Figure 1D**). However, high heterogeneity was observed in the exocytosis rate across cells (standard deviation of 0.15 Hz), indicating that there was strong cell-to-cell variability in secretion from the lysosomes.

Single cell spatial analysis to investigate whether exocytosis of lysosomes is random

It was possible to visualize the 2D distribution of exocytosis by KDE, as previously performed for endomembranous compartments[14], which could reveal differences in local densities (**Figure 2B**). This approach is pertinent for visualization of the average distribution of a population of cells, but less informative in single cells due to the limited number of events detected (tens versus the several thousand obtained by population-based analysis) and high cell-to-cell variability. For instance, this approach did not allow us to evaluate whether the distribution of exocytosis events followed a complete spatial randomness (CSR) behavior (i.e., corresponded to a uniform point distribution in an observed region for a single cell). A points pattern follows a CSR behavior when the two following hypotheses are true: 1) each point's location is independent of that of the other points; and 2) the probability to find a point in a subregion is only dependent on the ratio between this subregion's area and the total area. There are three possible deviations from CSR: 1) clustering (i.e., aggregation); 2) dispersion (i.e., ordering with constant distance); or 3) a mixture of clustering and dispersion (**Figure 2C**). Ripley's K function was used to answer this question as in previous analyses[7,8,9] (**Figure 2D**). Ripley's K function is close to πr^2 (with d being the normalized distance from an event) in the case of CSR, but superior (respiratory inferior) to πr^2 in the case of clustering (respiratory dispersion). By subtracting πr^2 from Ripley's K function, the theoretical CSR curve should be at 0. Simulations of CSR cases were performed using the same number of points as the observed exocytosis events to assess the goodness-of-fit for the CSR case (gray envelope around the theoretical curve). The transformed Ripley's K function applied to the experimental data exhibited positive values outside the envelope, indicating clustering (**Figure 2D**).

To investigate if clustering of exocytosis events was due to cell adhesion as previously reported[6], we performed a similar analysis on data from exclusively the nonadhesive cell area in the center (**Figure 2A**, adhesive area in gray, nonadhesive cell center area in white). Of note, we found that exocytosis events in the nonadhesive area were also clustered (**Figure 2E**), indicating that adhesion molecules were not the only structures that induced secretory hot spots at plasma membranes.

Because Ripley's K function is a descriptive statistic that does not provide a P value, a statistical test was set up comparing cellular exocytosis events with CSR simulations. The nearest neighbor distance NND(i) method was used. NDD is defined as the minimal Euclidian distance between a point i and all other points. The average NND(i) from all exocytic events of one cell was computed

and compared to CSR obtained with a high number of Monte Carlo simulations (**Figure 2F**). We found that the average NND of the single cell analyzed in **Figure 2F** was lower than the average of the simulated distribution of the CSR case, indicating closer neighbors on average and thus clustering. In the case of dispersion, a higher value for the average NND was expected (**Figure 2C**). This comparison allowed the calculation of a P value for each cell. The P value represents the percentage of simulations that exhibited a more extreme NND (in a two-sided way). To be precise, the unbiased P value was computed as (k+1)/(N+1) with N being the total number of Monte-Carlo simulations (10,000), and k the number of these simulations that was more extreme than the observed measurent[16]. The histogram of all P values was plotted for the total cell area (**Figure 2G**) and the nonadhesive cell area (**Figure 2I**). If H_0: "Exocytosis is a CSR process" was true, a uniform distribution of P values was expected. If H_0 was false, a peak at a low P value was expected. Performing a Kolmogorov-Smirnov test on the P value histograms, a P value inferior to 0.001 was obtained, showing a significant deviation from CSR in both cases (**Figures 2G** and **2I**). Moreover, a clustering coefficient of 0.955 for the total cell area and 1.000 for the nonadhesive cell area indicated that lysosomal exocytosis was a clustered process independent of cell adhesion. The clustering coefficient represents the percentage of cells that were closer to a clustering behavior than dispersion. This result was consistent with Ripley's K function.

To evaluate the role of cell adhesion in clustering, we compared the average NND in the nonadhesive area with that in the overall area for each individual cell (**Figure 2H**). Because the average NND was inversely proportional to the surface density, we normalized the average NND of the nonadhesive area using homothety. The significantly larger average NND of exocytosis events in the nonadhesive area indicated less clustering (**Figure 2H**). Thus, although secretion from lysosomes clusters in nonadhesive areas, cell adhesion seemed to enhance clustering.

Spatial analysis of exocytosis events using polar coordinates

The circular geometry of the ring-shaped micropattern allowed the use of the common polar coordinates, which simplified analyses, as previously found[17]. Each exocytosis event could thus be described by a modulus (distance from the origin, here the center of the lower plane of the cell) and an angle (according to a fixed arbitrary axis). Additionally, the modulus can be normalized by dividing it by the radius of the cell. The histogram of exocytosis events was plotted according to the modulus for a representative cell (**Figure 3A**). This revealed a peak around the border between the adhesive/nonadhesive areas. A large variability between cells was also observed. Therefore, we pooled n = 22 cells to obtain an average distribution of exocytosis events. However, in order to give the same statistical weight to each cell, the same number of events from each cell was randomly selected. This random selection did not change the overall patterns seen. To obtain a continuous average distribution of the individual distributions of single cells, a KDE was used (**Figure 3B**). However, because the normalized modulus is between 0 and 1, edge conditions had to be taken into consideration. A beta kernel that changes shape next to edges was used[18]. An error band was computed with a bootstrap strategy. The observed average distribution was compared to a hypothetical CSR distribution that showed more events at a higher modulus, because the area increased with a higher modulus. Because the integral of a probability density should be one, the CSR distribution was 2r (with r the normalized radius, without units). A confidence band was computed around the theoretical curve using a large

number of CSR Monte Carlo simulations (5,000 each). The 1st and 99th percentiles of the modulus distribution from these simulations were plotted. We found that the average distribution of exocytosis events deviated from the hypothetical one at $0.7r_{max}$, which corresponds to the beginning of the adhesive area of the cell.

We sought to test whether the observed distribution of the modulus was different from the theoretical one. Because average distributions, as in this case, cannot be accurately tested by a goodness-of-fit test (e.g., Kolmogorov-Smirnov) an alternative method proposed by Pecot et al. was employed. This method measures the difference between the variation across a population and the variation inside a population, and thus allows independent testing for each coordinate (i.e., modulus and angle)[17]. This test was used to compare our data to simulated data representing CSR exocytosis events (the same number of cells and exocytosis events as the observed data), and found a statistically significant difference in the variations ($p < 0.001$ with the Wilcoxon-Mann-Whitney test, $n = 22$ cells), indicating that the observed average exocytosis distribution was not CSR. However, when two CSR simulations (with 5,000 simulations each) were compared, we found that the P value histogram did not show a uniform distribution, but exhibited a peak near 1, indicating that this test probably lacked sensitivity.

Because the KDE estimation relies on a non-trivial choice of kernel bandwidth and is sensitive to edge effects, the cumulative distribution function was also computed, which overcomes the problems inherent in KDE estimation (**Figure 3D**). This function is defined between 0 and 1 and does not contain any arbitrary parameters or biases (e.g., edge biases). Error and confidence bands were computed in the same way as for the modulus distribution. The cumulative distribution function confirmed that exocytosis events did not follow a CSR distribution but were overconcentrated at moduli around $0.7r_{max}$. This analysis thus allowed us to identify cellular areas where clustering occurred. An interesting question that this result raises is whether the overconcentration at $0.7r_{max}$ was because of the presence of adhesive/nonadhesive areas of the ring-shaped micropattern or an effect of peripheral/central secretion areas of cells.

As the average distribution of exocytosis events deviated from the CSR case in nonadhesive as well as adhesive areas, we also wondered where the exocytosis density was highest. The surface densities of exocytosis in adhesion and nonadhesion areas were computed and compared. We found that the surface density was lower in the adhesion area than in the nonadhesion area by a paired analysis (**Figure 3C**). This could be explained by the strong decrease of exocytosis at the cell periphery ($0.85 – 1r_{max}$, **Figure 3B**).

FIGURE LEGENDS:

Figure 1. Exocytosis from lysosomes in hTert-RPE1 cells: (**A**) Ring-shaped micropattern (red) and adhesive hTert-RPE1 cell transfected with VAMP7-pHluorin (green) imaged by TIRFM. The arrow shows an exocytosis event. Scale bars = 10 µm. (**B**) Kymograph of exocytosis events. Arrows show exocytosis events. Scale bar = 2 µm, scale bar in time = 5 s. (**C**) Normalized intensity profile of lysosomal exocytosis from 22 cells. Each point is an average of at least 1,530 exocytosis events. Data are presented ± SEM. (**D**) Exocytosis rate of the 22 cells. The average +/- standard deviation is plotted in red.

Figure 2. Spatial analysis of lysosomal exocytosis events. (**A**) Scatter plot of exocytosis events during 5 min acquisition. Each dot represents one exocytosis event. The adhesive area is shown in gray. (**B**) 2D kernel density estimation (KDE) of scatter plot of **A**. The color represents the local density of exocytosis events. (**C**) Schematic representation of possible point patterns. The four cases, Complete Spatial Randomness (CSR), Clustering, Dispersion, and Mixed are shown, and several nearest neighbor distances (NND) are plotted (dashed lines) to show how the average NND decreased in clustering and increased with dispersion. (**D**) Analysis of one representative cell using Ripley's K function. The red dashed line equals "Ripley's K function - πr^2" for CSR events, the gray envelope represents the estimated goodness-of-fit from Monte Carlo simulations with the same number of points as exocytosis events ($N_{event} = 81$). The black solid line equals "Ripley's K function – πr^2" for observed exocytosis events ($N_{event} = 81$). Its positive deviation from the red curve out from the gray envelope indicates clustering of exocytosis events. Ripley's K function was normalized to have a maximum value of 1. (**E**) Analysis of the nonadhesive area of the same cell using Ripley's K function as in **D**. The positive deviation from the red curve outside the gray envelope indicates a clustering of exocytosis events in the nonadhesive area. (**F**) Comparison of the average NND distribution from one representative cell (red line) with the KDE of the CSR obtained from Monte Carlo simulations (blue curve). The P value was calculated as the percentage of simulated values that were more extreme than the value observed. (**G**) P value histogram obtained from the NND test as in **F** for n = 26 cells. The peak at low P values means that the null hypothesis "exocytosis follows CSR" was rejected with a Kolmogorov-Smirnov test, indicating that lysosomal exocytosis was not CSR. (**H**) Box-plot of average NND from exocytosis events in nonadhesive areas (white) and total cell areas (gray). The two data points from the same cell are joined by a line. The average NND was bigger in the nonadhesive area, $p < 0.001$ with a paired Wilcoxon test (n = 25 cells), indicating significantly less clustering in the nonadhesive area. (**I**) Same as **G** for the nonadhesive area for n = 26 cells.

Figure 3. Spatial analysis of pooled lysosomal exocytosis events: (**A**) Histogram of the exocytosis events of one representative cell during a 5 min acquisition with n = 161 exocytosis events as a function of the normalized modulus; 0 represents the cell center and 1 the cell periphery. The adhesive area of the cell is shown in gray and corresponds to moduli from 0.65–1 for the cells shown. There is a peak at the beginning of the adhesive area around moduli between 0.6 and 0.7. (**B**) KDE of the exocytosis events as a function of the normalized modulus for n = 22 cells with 56 events in each cell; 0 represents the cell center and 1 the cell periphery. The average adhesive area is shown in gray and corresponds on average to moduli from 0.61–1. The dashed blue curve is the theoretical curve expected in the case of CSR. This theoretical curve is accompanied by an envelope that represents the 1st–99th percentiles of CSR obtained using the Monte Carlo simulation. The KDE curve from the observed data is in red and accompanied by an error band generated by bootstrapping. The adhesive area is in gray +/- SEM. (**C**) Paired analysis of the surface densities in adhesion and nonadhesion areas. The exocytosis surface density was computed as the number of events per normalized area and per second. Here, $*p < 0.05$ from a paired student t-test (n = 22 cells). Normality was previously tested by a Shapiro-Wilk test. (**D**) Cumulative distribution function of the data in **B** (red line) and from Monte Carlo CSR simulations

(dotted blue line). Envelopes were generated as in **B**. Note that the red line deviates from the theoretical CSR at around $0.7r_{max}$.

DISCUSSION:

We monitored exocytosis events from the lysosomal compartment by TIRFM live cell imaging of VAMP7-pHluorin in ring-shaped micropattern-normalized cells and performed a rigorous statistical analysis of the spatial parameters of exocytosis events. Employing the transformed Ripley's K function and a statistical test based on the nearest neighbor distance, we confirmed that secretion from lysosomes is not a random process[8,9]. Both statistical analyses convincingly showed that exocytosis events exhibit clustering (**Figures 2D** and **2G**). Applying similar tools to the nonadhesive cell area, we found that exocytosis events are also clustered in nonadhesive areas (**Figures 2E** and **2I**). Thus, adhesion molecules that have been previously reported to allow clustering[6] are not the only structures that can induce secretory hot spots at the plasma membrane. However, cell adhesion enhanced clustering: the average nearest neighbor distance between exocytosis events was significantly larger in nonadhesive areas (**Figure 2H**). Consistently, our analysis based on kernel density estimation and the cumulative distribution function identified enriched areas of exocytosis that were located at the border between the adhesive and nonadhesive areas in ring-shaped micropattern cells. More work is necessary to determine the molecular mechanisms underlying clustering, such as adhesion or a specific targeting of lysosome to this region. Interestingly, we observed high heterogeneity in the exocytosis rate across hTERT-RPE1 cells (standard deviation of 0.15 Hz for average exocytosis rate of 0.28 Hz, **Figure 1D**), indicating that secretion from lysosomes has high intercellular variation. Therefore, subpopulation analyses should be considered in future work. It would be particularly interesting to investigate if this variation reflects the diversity of lysosomal compartments, differences in cargos, or dependence on exocytosis machinery.

These results illustrate how statistical tools can be employed to investigate spatial parameters of diverse biological processes. Moreover, micropatterns facilitate the study of the effect of cell adhesion in an unbiased manner with the help of different micropattern geometries (e.g., ring-shaped versus diskshaped). In particular, the use of round shapes facilitates analyses because polar coordinates can be employed. Because statistical tools require a certain amount of data to be meaningful, cells with more than 30 events were used for our analysis. However, there is a possibility that cells with 30 or fewer events are meaningful. Thus, sampling cells with 30 or fewer events could be performed in order to obtain sufficient events for analysis to determine if this is the case. Similarly, it is difficult to estimate how many cells should be analyzed, particularly if there is strong intercellular variation. One way to circumvent this is to randomly select the same number of events from each cell in order to give the same statistical weight to each cell when pooling them. However, we recommend that analyses on fewer than 15 cells be done with precaution. As average distributions of pooled cells cannot be accurately tested by goodness-of-fit tests (e.g., Kolmogorov-Smirnov) we employed a test statistic proposed by Pecot et al. that measures the difference in variations of populations[17]. Although this test allowed us to find a statistically significant difference in the variations in the average distributions, we suspect that this test has low sensitivity because the P value histogram was not flat (i.e., showed uniform

distribution) when comparing different CSR simulations for p values close to 1. Therefore, this statistical procedure may need to be improved.

One drawback to our analyses is the manual detection of exocytosis events, which drastically reduces the speed of the analysis. Limitations in automatic detection are often due to strong heterogeneity in the unique and simple parameter being analyzed (e.g., intensity of exocytosis events). Neural networks could be potentially powerful for automatic detection, because they can be trained to recognize many features.

The analysis presented here can be applied to other dynamic processes observed by TIRFM, such as secretion from other compartments and the distribution of the membrane microdomain or antigen presentation. Similar analyses can also be applied to fixed cells in order to study the spatial distribution of proteins. We hope that our work will enhance the increasing interest in spatial distribution analysis in cell biology.

ACKNOWLEDGMENTS:

We greatly acknowledge Thierry Galli (Center of Psychiatry and Neurosciences, INSERM) for providing the VAMP7-pHluorin plasmid. We thank Tarn Duong for advice on statistical analysis and members of the GOUD laboratory for fruitful discussions. The authors greatly acknowledge the Cell and Tissue Imaging Facility (PICT-IBiSA @Burg, PICT-EM @Burg and PICT-IBiSA @Pasteur) and Nikon Imaging Center, Institut Curie (Paris), member of the French National Research Infrastructure France-BioImaging (ANR10-INBS-04). H.L. was supported by the Association pour la Recherche sur le Cancer (ARC) and P.M. received funding from the European Union's Horizon 2020 research and innovation programme under Marie Skłodowska-Curie grant agreement No 666003. This work was supported by grants from INFECT-ERA (ANR-14-IFEC-0002-04), the Labex CelTisPhyBio (ANR-10-LBX-0038) and Idex Paris Sciences et Lettres (ANR-10-IDEX-0001-02 PSL), as well as the Centre National de la Recherche Scientifique and Institut Curie.

DISCLOSURES:

The authors have nothing to disclose.

REFERENCES:

1. Wu, L.-G., Hamid, E., Shin, W., Chiang, H.-C. Exocytosis and endocytosis: modes, functions, and coupling mechanisms. *Annual Review of Physiology*. **76**, 301–331 (2014).
2. Samie, M. A., Xu, H. Lysosomal exocytosis and lipid storage disorders. J*ournal of Lipid Research*. **55**, 995–1009 (2014).
3. Neher, E., Marty, A. Discrete changes of cell membrane capacitance observed under conditions of enhanced secretion in bovine adrenal chromaffin cells. *Proceedings of the National Academy of Sciences of the United States of America*. **79**, 6712–6716 (1982).
4. Grossier, J. P., Xouri, G., Goud, B., Schauer, K. Cell adhesion defines the topology of endocytosis and signalling. *The EMBO Journal.* **33,** 35–45 (2014).
5. Fourriere, L. et al. RAB6 and microtubules restrict protein secretion to focal adhesions. *Journal of Cell Biology.* **218**, 2215–2231 (2019).

6. Wang, Y., McNiven, M. A. Invasive matrix degradation at focal adhesions occurs via protease recruitment by a FAK-p130Cas complex. *Journal of Cell Biology*. **196**, 375–385 (2012).
7. Lagache, T., Lang, G., Sauvonnet, N., Olivo-Marin, J. C. Analysis of the spatial organization of molecules with robust statistics. *PLoS One*. **12**, e80914 (2013).
8. Yuan, T., Lu, J., Zhang, J., Zhang, Y., Chen, L. Spatiotemporal Detection and Analysis of Exocytosis Reveal Fusion "Hotspots" Organized by the Cytoskeleton in Endocrine Cells. *Biophysical Journal.* **108**, 251–260 (2015).
9. Urbina, F. L., Gomez, S. M., Gupton, S. L. Spatiotemporal organization of exocytosis emerges during neuronal shape change. *Journal of Cell Biology.* **217**, 1113–1128 (2018).
10. Martinez-Arca, S., Alberts, P., Zahraoui, A., Louvard, D., Galli, T. Role of Tetanus Neurotoxin Insensitive Vesicle-Associated Membrane Protein (Ti-Vamp) in Vesicular Transport Mediating Neurite Outgrowth. *Journal of Cell Biology*. **149**, 889–900 (2000).
11. Alberts, P. et al. Cdc42 and Actin Control Polarized Expression of TI-VAMP Vesicles to Neuronal Growth Cones and Their Fusion with the Plasma Membrane. *Molecular Biology of Cell.* **17**, 1194–1203 (2006).
12. Azioune, A., Storch, M., Bornens, M., Théry, M., Piel, M. Simple and rapid process for single cell micro-patterning. *Lab on a Chip.* **9***,* 1640–1642 (2009).
13. Baddeley, A. Rubak, E., Turner, R. *Spatial point Patterns: Methodology and Applications with R*. CRC Press, Indianapolis, IN. (2015).
14. Schauer, K. et al. Probabilistic density maps to study global endomembrane organization. *Nature Methods.* **7,** 560–566 (2010).
15. Advani, R.J. et al. Seven Novel Mammalian SNARE Proteins Localize to Distinct Membrane Compartments. *Journal of Biological Chemistry.* **273,** 10317–10324 (1998).
16. North, B. V., Curtis, D., Sham, P. C. A Note on the Calculation of Empirical P Values from Monte Carlo Procedures. *American Journal of Human Genetics*. **71**, 439–441 (2002).
17. Pecot, T., Zengzhen, L., Boulanger, J., Salamero, J., Kervrann, C. A quantitative approach for analyzing the spatio-temporal distribution of 3D intracellular events in fluorescence microscopy. *eLife.* **7,** e32311 (2018).
18. Chen, S. X. Beta kernel estimators for density functions. *Computational Statistics & Data Analysis.* **31**, 131–145 (1999).

Click here to access/download;Figure;Figure 1.pdf

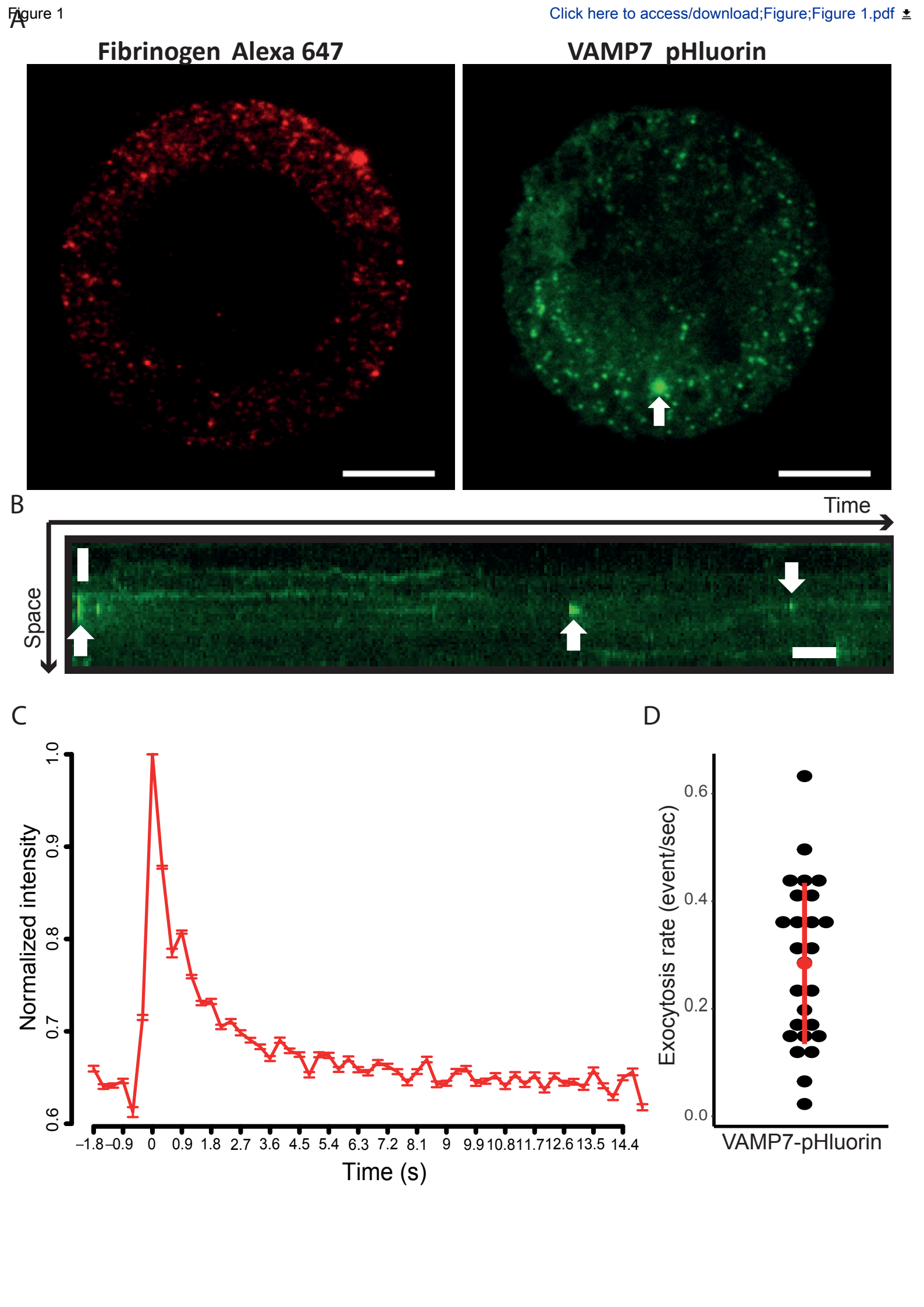

Figure 2

Click here to access/download;Figure;Figure 2.pdf

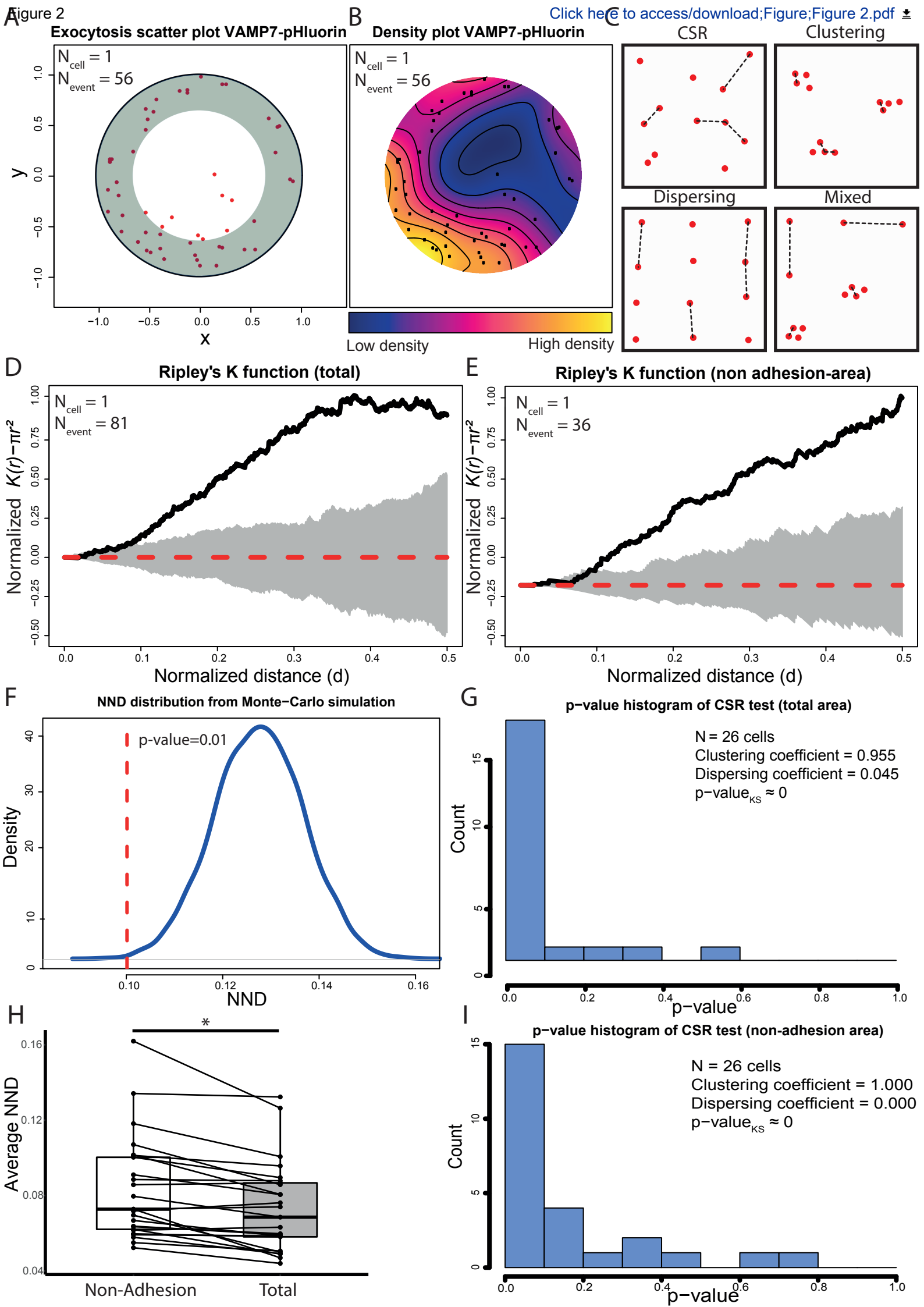

Figure 3

Click here to access/download;Figure;Figure 3.pdf

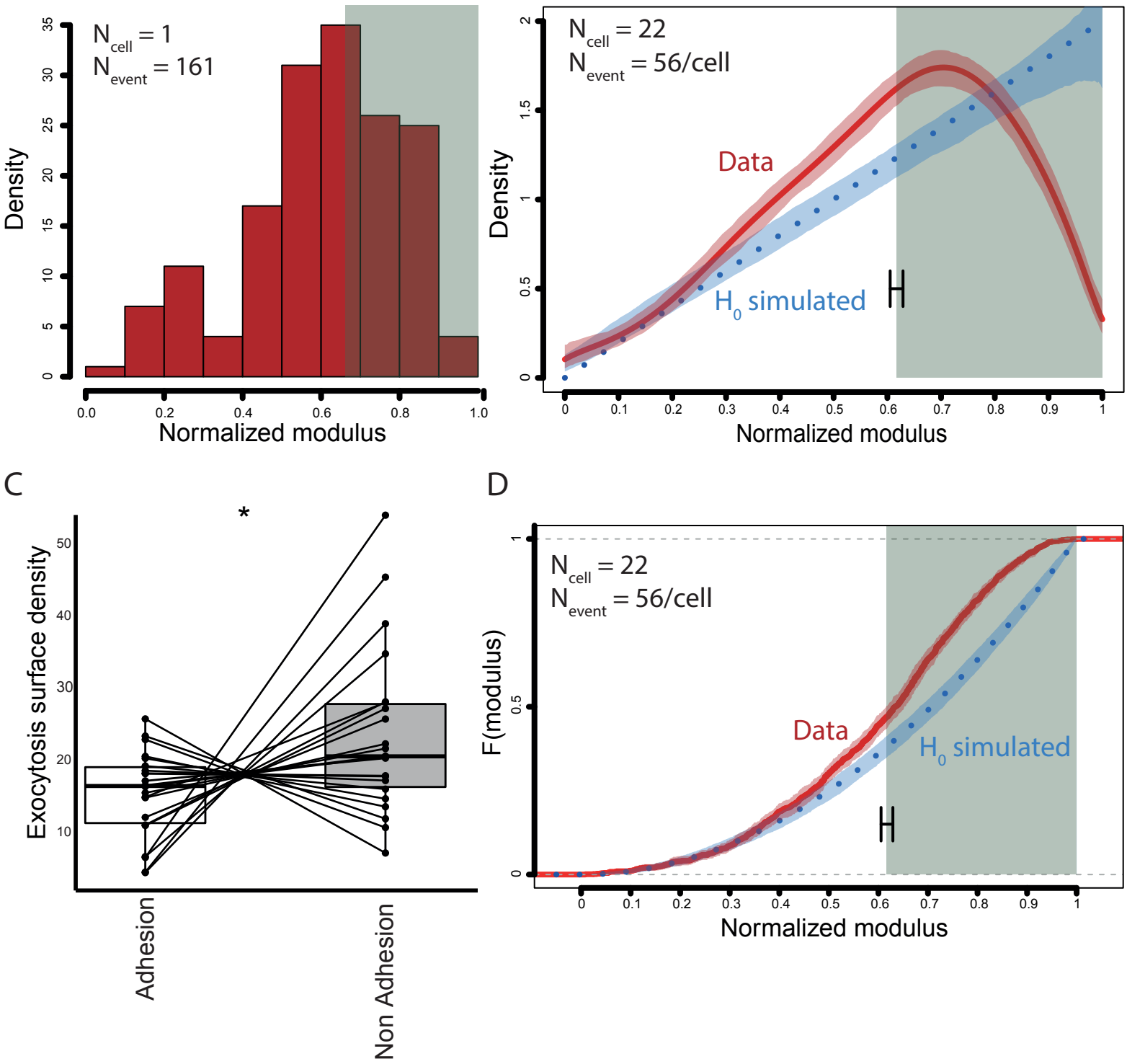

Click here to access/download;Table of Materials;JoVE_Materials.xls

Name of Material/ Equipment	Company	Catalog Number
Chamlide Magnetic Chamber	Chamlide	
DMEM/F12	Gibco	21041-025
Fibrinogen	Molecular Probes, Invitrogen	F35200
Fibronectin bovine plasma	Sigma	F1141
HEPES (1M)	Gibco	15630-056
hTert RPE1 cell line	https://www.atcc.org	
ImageJ	http://rsbweb.nih.gov/ij/	n/a
JetPRIME Transfection reagent	Polyplus	114-07
Penicilin/Streptomycin	Gibco	15140-122
Photomask	Delta Mask	
PLL-g-PEG solution	Surface Solutions	PLL(20)-g[3.5]- PEG(2)
R Software	https://www.r-project.org/	n/a
Trypsin (TrypLE Express 1X)	Gibco	12605-010
UV ozone oven	Jelight Company Inc	342-220
VAMP7-pHFluorin plasmid	n/a	n/a

Comments/Description

Authored by W. Rasband, NIH/NIMH

Paper reference :http://www.ncbi.nlm.nih.gov/pubmed/?term=Role+of+HRB+in+clathrin-dependent+endocytosis.

J Biol Chem. 2008 Dec 5;283(49):34365-73. doi: 10.1074/jbc.M804587200.

Role of HRB in clathrin-dependent endocytosis.

Chaineau M, Danglot L, Proux-Gillardeaux V, Galli T.

Rebuttal Letter

Click here to access/download;Rebuttal Letter;Rebuttle_letter_Final_2.docx

institutCurie
Ensemble, prenons le cancer de vitesse.

Paris, December 17th, 2019

Dear editor,

Please find enclosed a revised version of our manuscript JoVE60801R1 - "Quantifying spatio-temporal parameters of cellular exocytosis in micropatterned cells".

We thank the editor and reviewers for their valid remarks to improve the manuscript. We have addressed their remaining concerns and hope that our manuscript will now be suitable for publication in JoVE. Please find below a point-by-point response to the reviewers' comments.

Best regards,

Kristine Schauer

Editorial comments:

1. The editor has formatted the manuscript to match the journal's style. Please use the attached version for further revision.

2. Please address all the specific comments marked in the manuscript.

3. Once done please ensure that the highlight is no more than 2.75 pages including headings and spacings.

All these points have been addressed.

Reviewers' comments:

Reviewer #1:

Manuscript Summary:

The authors use a statistical approach (Ripley's K function and a statistical test based on nearest neighbor distance) to study the localization of secretion from lysosomes. They demonstrate that these events cluster together and therefore do not appear randomly in the cell. Their localization is correlated with the cell adhesion, even though they show that exocytosis events also clustered in non-adhesion areas.

The biological application is well suited to the protocol and makes this paper interesting to read. The statistical tools are relevant and useful for a wide range of applications in biological image processing.

Major Concerns:

The authors have addressed most of my previous concerns. However, they haven't addressed my second major concern (the fact that the use of polar coordinates is well suited to the study of cells with micropatterns is not new). For instance, they changed the R program that seems to be much more easy to use now, but I would have liked to know why they don't try to do everything with ImageJ for example.

We are sorry that our clarification that we do not claim novelty for the use of polar coordinates did not convince the reviewer. To even more show our effort we have added a reference, in which polar coordinates were used previously to unambiguously show that we do not claim novelty. This has been added on page 8: "The circular geometry of the ring-shaped

micropattern allows the use of the common polar coordinates, which simplifies analyses such as previously performed[17]."

We do not use ImageJ for the analysis, because ImageJ is not well suited for statistical analysis as it does not provide pre-coded packages for instance for spatial statistics. This means that all analysis needs to be coded that is time consuming and not efficient. ImageJ is primary a program to handle images and extract data from them. On the other hand, a powerful tool for statistical analysis is R that provided many interesting packages and that in addition is much easier to use for scientists who would like to change the code or further analyze data.

Reviewer #2:

Major Concerns:
Most of my comments have appropriately been considered. However, I still do not understand the passage on lines 435-440 in the light of Fig. 3B. The authors interpret the data by the strong decrease of exocytosis at the cell periphery. In the figure the experimental curve is in the adhesive ring first above and then below the CSR reference. I cannot see how in this case the effect of adhesive / non-adhesive can be distinguished from peripheral / central. I think that two identical halves of a cell, one on adhesive the other on non-adhesive substrate, should be compared to evaluate the effect of adhesiveness.

We agree with the referee. We cannot distinguish between an adhesion versus peripheral effect. Indeed, we have performed other experiments to further test the role of adhesion versus peripheral effects and find that round patterns on which cells can adhere on the entire area do not show an over-concentration at $0.7r_{max}$. However, we do not want to present these results in the manuscript, because they need further biological experiments that is out of the scope of this methodological paper. However, we have added the following sentence to the discussion on page 9 to raise awareness for this valid point: "An interesting question which raises this result is whether the over-concentration at $0.7r_{max}$ is because of the presence of adhesive / non-adhesive areas of the ring-shaped micropattern or an effect of peripheral / central secretion areas of cells."

Additionally, we have modified Figure 3B. to facilitate interpretation.

Minor Concerns:

Typos:
Line 142: coverslip
Line 267: length by (or through) dividing?

The typos have been corrected.

Reviewer #3:

Manuscript Summary:
"This article presents a very interesting, statistically based methodology for studying lysosomal exocytosis making use of TIRF microscopy on cells attached by means of circular symmetric micro patterns. Although I am convinced that less sophisticated methods based only on spatial density of the fluorescence spots and near Neighbour distance (NND) would suffice to achieve the same results the approach described is in general solid, high quantitative as well as correct."

Major Concerns:

I acknowledge the improvements and corrections made in the protocol and in the text; however I am still convinced that the paper in its current form does not show a really usable protocol to be published in JoVE. To reverse this statement the authors should have followed my previous indications or at least should have explained why this is not possible. In general I still have one main concern:

1) The protocol, in the way it is made and presented appears to be unpractical and unusable in a scientific lab (thus not respecting JoVE guidelines). This important point comes from the first review process and kept mainly unchanged:

Once I install the open source program, the extra packages and run the script many pdf pictures were generated displaying all data as it was presented in Figure 2 and 3 of this paper. It is still not given the opportunity to access the computed results in numerical format in order to use them later for plotting or extracting relevant numbers. In my opinion this protocol should not be accepted for publication in JoVE if the authors keep this protocol in an undoable form. To make this part and thus the entire protocol publishable in JoVE I suggest that the authors modify their script. The modified script should automatically produce and save in addition to the pdfs files also the same data in numerical format i.e.

(.txt) in a way that the users can access and work independently on their datasets.

Since this point is almost entirely copied and pasted from the first review I ask myself what is the problem in implementing this modification: is it too demanding write few lines more of code? Or does the program not allow doing so? Clearly the users for whom this program is designed will not wish to learn it all from scratch and implement themselves if applicable these modifications.

It is up to the editor to decide if a protocol made for data analysis is complete and publishable when it provides the results of the analysis in a not editable way.

We are very sorry that we did not understand the concern of the referee during the first revision. We have now modified the packages to provide txt files containing data in addition to visual outputs. The txt files are:
-Normalized polar and Cartesian coordinates for each cell
-The density of events in adhesion and no adhesion area for each cell
-The observed mean and standard deviation NND for each cell; and the mean and standard deviation of simulated NND; and the p-value associated
-The same but only for non-adhesion area.
-Statistics of the paired NND analysis

For other plots (density and Ripley's K function for example), we cannot give a txt files with all numerical values but the user can easily replot it from txt files (especially the ones with coordinates). Indeed, we hope that users will use the data from the analysis to work further on them. Moreover, we hope that in the current form the code can be easily modified in R for further analysis (see also response to referee #1).

Another issue I would like to note is that instead of making a quantitative argumentation between lines 543-548 the authors keep defending their "human based detection method" simply stating that human eyes work better than automatic spot detection routine. In light microscopy this is clearly not true: Human eyes are clearly less accurate in detecting and localizing light sparks. If the authors cannot change their minds or quantitatively demonstrate their statements they can at least abolish lines 453-458.

This is an empirical observation in our laboratory. We agree that it is possible for a computer to do as good as a human but it is not a simple problem to establish a program that can identify exocytosis events in a robust manner. So far, we were not able to write a good

program for automated exocytosis detection. We would like to emphasize that detection of exocytosis is not similar to spot detection because exocytosis events have a temporal pattern, and thus it is impossible to detect exocytosis from a single image. We have however abolished the text on page 12 as proposed by the referee.

Click here to access/download;Author License Agreement (ALA);JoVE60801 (1).pdf

1 Alewife Center #200
Cambridge, MA 02140
tel. 617.945.9051
www.jove.com

ARTICLE AND VIDEO LICENSE AGREEMENT

Title of Article:	Quantifying spatio-temporal parameters of cellular exocytosis in micropatterned cells
Author(s):	Hugo Lachuer, Pallavi Mathur, Kevin Bleakley, Kristine Schauer

Item 1: The Author elects to have the Materials be made available (as described at http://www.jove.com/publish) via:

☑ Standard Access ☐ Open Access

Item 2: Please select one of the following items:

☑ The Author is **NOT** a United States government employee.

☐ The Author is a United States government employee and the Materials were prepared in the course of his or her duties as a United States government employee.

☐ The Author is a United States government employee but the Materials were NOT prepared in the course of his or her duties as a United States government employee.

ARTICLE AND VIDEO LICENSE AGREEMENT

1. **Defined Terms.** As used in this Article and Video License Agreement, the following terms shall have the following meanings: "**Agreement**" means this Article and Video License Agreement; "**Article**" means the article specified on the last page of this Agreement, including any associated materials such as texts, figures, tables, artwork, abstracts, or summaries contained therein; "**Author**" means the author who is a signatory to this Agreement; "**Collective Work**" means a work, such as a periodical issue, anthology or encyclopedia, in which the Materials in their entirety in unmodified form, along with a number of other contributions, constituting separate and independent works in themselves, are assembled into a collective whole; "**CRC License**" means the Creative Commons Attribution-Non Commercial-No Derivs 3.0 Unported Agreement, the terms and conditions of which can be found at: http://creativecommons.org/licenses/by-nc-nd/3.0/legalcode; "**Derivative Work**" means a work based upon the Materials or upon the Materials and other pre-existing works, such as a translation, musical arrangement, dramatization, fictionalization, motion picture version, sound recording, art reproduction, abridgment, condensation, or any other form in which the Materials may be recast, transformed, or adapted; "**Institution**" means the institution, listed on the last page of this Agreement, by which the Author was employed at the time of the creation of the Materials; "**JoVE**" means MyJove Corporation, a Massachusetts corporation and the publisher of The Journal of Visualized Experiments; "**Materials**" means the Article and / or the Video; "**Parties**" means the Author and JoVE; "**Video**" means any video(s) made by the Author, alone or in conjunction with any other parties, or by JoVE or its affiliates or agents, individually or in collaboration with the Author or any other parties, incorporating all or any portion of the Article, and in which the Author may or may not appear.

2. **Background.** The Author, who is the author of the Article, in order to ensure the dissemination and protection of the Article, desires to have the JoVE publish the Article and create and transmit videos based on the Article. In furtherance of such goals, the Parties desire to memorialize in this Agreement the respective rights of each Party in and to the Article and the Video.

3. **Grant of Rights in Article.** In consideration of JoVE agreeing to publish the Article, the Author hereby grants to JoVE, subject to **Sections 4** and **7** below, the exclusive, royalty-free, perpetual (for the full term of copyright in the Article, including any extensions thereto) license (a) to publish, reproduce, distribute, display and store the Article in all forms, formats and media whether now known or hereafter developed (including without limitation in print, digital and electronic form) throughout the world, (b) to translate the Article into other languages, create adaptations, summaries or extracts of the Article or other Derivative Works (including, without limitation, the Video) or Collective Works based on all or any portion of the Article and exercise all of the rights set forth in (a) above in such translations, adaptations, summaries, extracts, Derivative Works or Collective Works and(c) to license others to do any or all of the above. The foregoing rights may be exercised in all media and formats, whether now known or hereafter devised, and include the right to make such modifications as are technically necessary to exercise the rights in other media and formats. If the "Open Access" box has been checked in **Item 1** above, JoVE and the Author hereby grant to the public all such rights in the Article as provided in, but subject to all limitations and requirements set forth in, the CRC License.

4. **Retention of Rights in Article.** Notwithstanding the exclusive license granted to JoVE in **Section 3** above, the Author shall, with respect to the Article, retain the non-exclusive right to use all or part of the Article for the non-commercial purpose of giving lectures, presentations or teaching classes, and to post a copy of the Article on the Institution's website or the Author's personal website, in each case provided that a link to the Article on the JoVE website is provided and notice of JoVE's copyright in the Article is included. All non-copyright intellectual property rights in and to the Article, such as patent rights, shall remain with the Author.

5. **Grant of Rights in Video – Standard Access.** This **Section 5** applies if the "Standard Access" box has been checked in **Item 1** above or if no box has been checked in **Item 1** above. In consideration of JoVE agreeing to produce, display or otherwise assist with the Video, the Author hereby acknowledges and agrees that, Subject to **Section 7** below, JoVE is and shall be the sole and exclusive owner of all rights of any nature, including, without limitation, all copyrights, in and to the Video. To the extent that, by law, the Author is deemed, now or at any time in the future, to have any rights of any nature in or to the Video, the Author hereby disclaims all such rights and transfers all such rights to JoVE.

6. **Grant of Rights in Video – Open Access.** This **Section 6** applies only if the "Open Access" box has been checked in **Item 1** above. In consideration of JoVE agreeing to produce, display or otherwise assist with the Video, the Author hereby grants to JoVE, subject to **Section 7** below, the exclusive, royalty-free, perpetual (for the full term of copyright in the Article, including any extensions thereto) license (a) to publish, reproduce, distribute, display and store the Video in all forms, formats and media whether now known or hereafter developed (including without limitation in print, digital and electronic form) throughout the world, (b) to translate the Video into other languages, create adaptations, summaries or extracts of the Video or other Derivative Works or Collective Works based on all or any portion of the Video and exercise all of the rights set forth in (a) above in such translations, adaptations, summaries, extracts, Derivative Works or Collective Works and (c) to license others to do any or all of the above. The foregoing rights may be exercised in all media and formats, whether now known or hereafter devised, and include the right to make such modifications as are technically necessary to exercise the rights in other media and formats. For any Video to which this **Section 6** is applicable, JoVE and the Author hereby grant to the public all such rights in the Video as provided in, but subject to all limitations and requirements set forth in, the CRC License.

7. **Government Employees.** If the Author is a United States government employee and the Article was prepared in the course of his or her duties as a United States government employee, as indicated in **Item 2** above, and any of the licenses or grants granted by the Author hereunder exceed the scope of the 17 U.S.C. 403, then the rights granted hereunder shall be limited to the maximum rights permitted under such statute. In such case, all provisions contained herein that are not in conflict with such statute shall remain in full force and effect, and all provisions contained herein that do so conflict shall be deemed to be amended so as to provide to JoVE the maximum rights permissible within such statute.

8. **Protection of the Work.** The Author(s) authorize JoVE to take steps in the Author(s) name and on their behalf if JoVE believes some third party could be infringing or might infringe the copyright of either the Author's Article and/or Video.

9. **Likeness, Privacy, Personality.** The Author hereby grants JoVE the right to use the Author's name, voice, likeness, picture, photograph, image, biography and performance in any way, commercial or otherwise, in connection with the Materials and the sale, promotion and distribution thereof. The Author hereby waives any and all rights he or she may have, relating to his or her appearance in the Video or otherwise relating to the Materials, under all applicable privacy, likeness, personality or similar laws.

10. **Author Warranties.** The Author represents and warrants that the Article is original, that it has not been published, that the copyright interest is owned by the Author (or, if more than one author is listed at the beginning of this Agreement, by such authors collectively) and has not been assigned, licensed, or otherwise transferred to any other party. The Author represents and warrants that the author(s) listed at the top of this Agreement are the only authors of the Materials. If more than one author is listed at the top of this Agreement and if any such author has not entered into a separate Article and Video License Agreement with JoVE relating to the Materials, the Author represents and warrants that the Author has been authorized by each of the other such authors to execute this Agreement on his or her behalf and to bind him or her with respect to the terms of this Agreement as if each of them had been a party hereto as an Author. The Author warrants that the use, reproduction, distribution, public or private performance or display, and/or modification of all or any portion of the Materials does not and will not violate, infringe and/or misappropriate the patent, trademark, intellectual property or other rights of any third party. The Author represents and warrants that it has and will continue to comply with all government, institutional and other regulations, including, without limitation all institutional, laboratory, hospital, ethical, human and animal treatment, privacy, and all other rules, regulations, laws, procedures or guidelines, applicable to the Materials, and that all research involving human and animal subjects has been approved by the Author's relevant institutional review board.

11. **JoVE Discretion.** If the Author requests the assistance of JoVE in producing the Video in the Author's facility, the Author shall ensure that the presence of JoVE employees, agents or independent contractors is in accordance with the relevant regulations of the Author's institution. If more than one author is listed at the beginning of this Agreement, JoVE may, in its sole

discretion, elect not take any action with respect to the Article until such time as it has received complete, executed Article and Video License Agreements from each such author. JoVE reserves the right, in its absolute and sole discretion and without giving any reason therefore, to accept or decline any work submitted to JoVE. JoVE and its employees, agents and independent contractors shall have full, unfettered access to the facilities of the Author or of the Author's institution as necessary to make the Video, whether actually published or not. JoVE has sole discretion as to the method of making and publishing the Materials, including, without limitation, to all decisions regarding editing, lighting, filming, timing of publication, if any, length, quality, content and the like.

12. **Indemnification.** The Author agrees to indemnify JoVE and/or its successors and assigns from and against any and all claims, costs, and expenses, including attorney's fees, arising out of any breach of any warranty or other representations contained herein. The Author further agrees to indemnify and hold harmless JoVE from and against any and all claims, costs, and expenses, including attorney's fees, resulting from the breach by the Author of any representation or warranty contained herein or from allegations or instances of violation of intellectual property rights, damage to the Author's or the Author's institution's facilities, fraud, libel, defamation, research, equipment, experiments, property damage, personal injury, violations of institutional, laboratory, hospital, ethical, human and animal treatment, privacy or other rules, regulations, laws, procedures or guidelines, liabilities and other losses or damages related in any way to the submission of work to JoVE, making of videos by JoVE, or publication in JoVE or elsewhere by JoVE. The Author shall be responsible for, and shall hold JoVE harmless from, damages caused by lack of sterilization, lack of cleanliness or by contamination due to the making of a video by JoVE its employees, agents or independent contractors. All sterilization, cleanliness or decontamination procedures shall be solely the responsibility of the Author and shall be undertaken at the Author's expense. All indemnifications provided herein shall include JoVE's attorney's fees and costs related to said losses or damages. Such indemnification and holding harmless shall include such losses or damages incurred by, or in connection with, acts or omissions of JoVE, its employees, agents or independent contractors.

13. **Fees.** To cover the cost incurred for publication, JoVE must receive payment before production and publication of the Materials. Payment is due in 21 days of invoice. Should the Materials not be published due to an editorial or production decision, these funds will be returned to the Author. Withdrawal by the Author of any submitted Materials after final peer review approval will result in a US$1,200 fee to cover pre-production expenses incurred by JoVE. If payment is not received by the completion of filming, production and publication of the Materials will be suspended until payment is received.

14. **Transfer, Governing Law.** This Agreement may be assigned by JoVE and shall inure to the benefits of any of JoVE's successors and assignees. This Agreement shall be governed and construed by the internal laws of the Commonwealth of Massachusetts without giving effect to any conflict of law provision thereunder. This Agreement may be executed in counterparts, each of which shall be deemed an original, but all of which together shall be deemed to me one and the same agreement. A signed copy of this Agreement delivered by facsimile, e-mail or other means of electronic transmission shall be deemed to have the same legal effect as delivery of an original signed copy of this Agreement.

A signed copy of this document must be sent with all new submissions. Only one Agreement is required per submission.

CORRESPONDING AUTHOR

Name:	Kristine Schauer
Department:	UMR144
Institution:	Institut Curie
Title:	CR CNRS

Signature: Kristine Schauer Date: 09/19/2019

Please submit a **signed** and **dated** copy of this license by one of the following three methods:

1. Upload an electronic version on the JoVE submission site
2. Fax the document to +1.866.381.2236
3. Mail the document to JoVE / Attn: JoVE Editorial / 1 Alewife Center #200 / Cambridge, MA 02140

Signature Certificate

Document Ref.: PRMIW-HF3GV-GYRFY-P9QQD

Document signed by:

Kristine Schauer

Verified E-mail:
kristine.schauer@curie.fr

IP: 86.246.20.116 | Date: 19 Sep 2019 15:34:07 UTC

Kristine Schauer

Document completed by all parties on:
19 Sep 2019 15:34:07 UTC

Signed with PandaDoc.com

PandaDoc is the document platform that boosts your company's revenue by accelerating the way it transacts.